On DEF expansion modelling in concrete structures under variable hydric conditions

Marie Malbois, Boumediene Nedjar, Stéphane Lavaud, Claude Rospars, Loïc Divet, Jean Michel Torrenti

On DEF expansion modelling in concrete structures under variable hydric conditions

M. Malbois[a], B. Nedjar[b,*], S. Lavaud[b], C. Rospars[b], L. Divet[b], J.-M. Torrenti[b]

[a] *Laboratoire de Mécanique et Technologie - ENS Cachan*
61, Avenue du Président Wilson, 94235 Cachan Cedex, France
[b] *Université Paris-Est, IFSTTAR/MAST*
14-20, Boulevard Newton, Cité Descartes, 77447 Marne-la-Vallée Cedex 2, France

Abstract

Delayed Ettringite Formation (DEF) in concrete is likely to develop in massive civil engineering structures such as bridges, nuclear plants, and dams with major security issues. In many cases, DEF pathology can lead to swelling and cracking which may significantly impact mass transfer and mechanical properties. It is then of major importance to build predictive tools for engineering conceptions and expertises. In this contribution, the chemical swelling evolution is integrated within the overall constitutive law of concrete that, besides, can experience other phenomena such like damage, plasticity, and long term creep, not all considered here. On another hand, as DEF is activated by environmental humidity above a certain threshold, we introduce the notion of effective time that takes into account the cumulative exposition above this threshold. Hence, a special care is taken with regards to the chem-

*Corresponding author
Email addresses: malbois@lmt.ens-cachan.fr (M. Malbois), boumediene.nedjar@ifsttar.fr (B. Nedjar), stephane.lavaud@ifsttar.fr (S. Lavaud), claude.rospars@ifsttar.fr (C. Rospars), loic.divet@ifsttar.fr (L. Divet), jean-michel.torrenti@ifsttar.fr (J.-M. Torrenti)

ical irreversibility, together with the humidity-drying cycles. Computations are used to calibrate various sets of model parameters with the help of results from the literature, on the one hand, and from an experimental campaign where a calcareous aggregates-based concrete is studied, on the other hand. We show the efficiency of the developed numerical tool through a series of numerical examples.

Keywords: DEF pathology modelling, Variable humidity, Effective time concept

---

1. Introduction

Delayed ettringite formation (DEF) in concrete can have significant impact on the long term behaviour of massive concrete structures. The swelling induced by the development of this pathology generates cracking and so can in general affect the mechanical properties, the transfer properties, for instance see [1, 2], and the durability of the concrete structures, for instance [3]. It is then of major importance to build numerical tools that can simulate this expanding kinematics and its consequences on the structural serviceability. Ettringite formation is delayed under a particular set of conditions, that have been unequally thoroughly studied: cement compositions ([4],[5],[6],[7] among others), aggregate mineralogical nature ([8],[9],[10],[11], among others), curing ([12],[13],[7]) or environmental humidity. Few authors have focused on the study the influence of the ambient humidity of the material. Water has a significant role in the delayed ettringite formation. It has been noticed that the concrete structures with DEF pathology were in an environment with a high ambient relative humidity (submerged parts, inflows of

water, or exposition to high humidity). Water seems to be both a reaction agent and environment, as ettringite crystallisation requires 32 molecules of water ([14]), but it also allows the transport of other agents that influence the formation of DEF ([15]). Indeed, it boosts the leaching of alkalines out of the interstitial water in the material, leading to a decrease of pH which favours the formation of ettringite. It is nowadays unanimously accepted that the DEF rate and amplitude is increased by the increase of saturated water, thus environmental humidity, e.g. see for example [16], [15], [17], [18], [19]. For instance in [17] and [19], the authors have even demonstrated experimentally this impact by putting reactive mortar and concrete in different controlled environments from 75%RH to 100%RH. Based on macroscopic observations, they identified a RH threshold of about 92% to initiate DEF.

From the mathematical point of view, extensive research has been conducted to model expansions caused by DEF, see for example [18, 13, 20, 21, among others] where expansions range around 0.25% to 1.3%, even, up to 3% [22], and further developments are nowadays still ongoing. The models are mostly based on phenomenological approaches formulated in terms of internal variables. The expansion is in general characterized by two important ingredients:

(i) An amplitude that depends on the temperature history at early age due to hydration and/or on heating conditions if a curing process is employed such as for pre-casting;

(ii) A kinetics that depends on the time, more precisely on the cumulated time, of exposure in contact with water.

Of interest in this work is the introduction of a new notion; the concept of *effective* time, that we denote throughout by $\widetilde{t}$, and that is controlled by the amount of water (humidity) during time and, consequently, that influences the kinetics of expansion, i.e. the above ingredient (ii). This extends the applicability of the existing expansion models not only for cases of full saturation, but for varying environmental conditions as well. Among others, the effective time depends on a threshold below which the swelling process stops, and above which swelling strongly depends on humidity as well as on temperature. Within the continnum, the effective time is an internal field variable since each material point $\boldsymbol{x}$ has its own humidity history during the real time t; $\widetilde{t} \equiv \widetilde{t}(\boldsymbol{x}, t)$.

An outline of the remainder of this paper is as follows: we first recall the basic constitutive equations together with the kinematical assumption we adopt in this work. The notion of effective time is then motivated and detailed with a focus on the most relevant points involved by the present formulation. Finally, we present a set of numerical simulations to illustrate the effectiveness of the proposed framework that compare satisfactorily against experimental data from an experimental campaign and from results in the literature.

2. Swelling kinematrics

The kinematical choice is as usual based on an additive split of the *total* strain tensor $\boldsymbol{\varepsilon}$ into an elastic part $\boldsymbol{\varepsilon}^{\mathrm{e}}$ and complementary parts, each one corresponding to a phenomenon. To be as clear as possible, let us consider

the simplest choice,

$$\boldsymbol{\varepsilon} = \boldsymbol{\varepsilon}^{\mathrm{e}} + \boldsymbol{\varepsilon}_{\mathrm{th}} + \boldsymbol{\varepsilon}_{\mathrm{hyd}} + \boldsymbol{\varepsilon}_{\chi} \ , \tag{1}$$

where $\boldsymbol{\varepsilon}_{\mathrm{th}}$ and $\boldsymbol{\varepsilon}_{\mathrm{hyd}}$ are respectively the thermal and hydric dilatations, and $\boldsymbol{\varepsilon}_{\chi}$ the chemical expansion tensor, in our case due to DEF. We can use the classical relations for the formers as:

$$\boldsymbol{\varepsilon}_{\mathrm{th}} = \alpha \left(T - T_0\right) \mathbf{1} \ , \quad \boldsymbol{\varepsilon}_{\mathrm{hyd}} = \varpi \left(S_r - S_{r0}\right) \mathbf{1} \ , \tag{2}$$

where T is the temperature, S_r is the saturation, α and ϖ are respectively the thermal and hydric dilatation coefficients, assumed constant for simplicity, and $\mathbf{1}$ is the second-order identity tensor. Here T_0 and S_{r0} are the initial temperature and the initial saturation, respectively. Notice that a form based on the relative humidity can equivalently be used instead of the saturation-based form $(2)_2$. In future contributions, inelastic deformations through a plastic strain $\boldsymbol{\varepsilon}^{\mathrm{p}}$ together with creep through a viscoelastic strain $\boldsymbol{\varepsilon}^{\mathrm{v}}$ will be appended to the decomposition (1) in a classical fashion, i.e. $\boldsymbol{\varepsilon} \equiv \boldsymbol{\varepsilon}^{\mathrm{e}} + \boldsymbol{\varepsilon}_{\mathrm{th}} + \boldsymbol{\varepsilon}_{\mathrm{hyd}} + \boldsymbol{\varepsilon}_{\chi} + \boldsymbol{\varepsilon}^{\mathrm{p}} + \boldsymbol{\varepsilon}^{\mathrm{v}}$, see for example [23, 24] for similar couplings.

Now if we consider a purely volumetric chemical expansion, we write:

$$\boldsymbol{\varepsilon}_{\chi} = \varepsilon_{\chi} \mathbf{1} \ , \tag{3}$$

where the scalar functional $\varepsilon_{\chi} \equiv \varepsilon_{\chi}(S_r, T, t \ldots)$ is the so-called free chemical expansion, the expression of which depends on the humidity, the temperature, and of course on the time as well.

In fully saturated conditions ($S_r = 1$ all the time), one has the nowadays well known expression used for both of DEF and Alkali-Aggregate Reaction

(AAR) expansions phenomena, see for example [10, 25, 18, among others] :

$$\varepsilon_\chi = \varepsilon_\infty^0 \, \frac{1 - e^{\left(-\frac{t}{\tau_c}\right)}}{1 + e^{\left(-\frac{t-\tau_l}{\tau_c}\right)}} \left(1 - \frac{\phi}{t+\delta}\right) , \tag{4}$$

where,

- ε_∞^0 is the potential chemical strain that constitues the amplitude of expansion, i.e. ingredient (i) in the Introduction Section,
- τ_c and τ_l are respectively the characteristic and latent times that characterize the kinetics of expansion,
- and ϕ and δ are parameters that control the long term kinetics. They are such that $\delta > \phi$. Equation (4) reduces to Larive's law [26] when ϕ is set to zero.

For the case of a DEF analysis, ε_∞^0 depends on the thermal history at *early-age*. To fix the ideas the following definition can be used for its modelling, see for instance [25, 27]:

$$\varepsilon_\infty^0 = \bar{\alpha} \int_0^{t_\mathrm{m}} \begin{cases} 0 \ \mathrm{d}t \ , & \text{if } T \leq T_\mathrm{def} \\ e^{\left[-\frac{E_a^\mathrm{def}}{R} \, \frac{1}{T - T_\mathrm{def}}\right]} \ \mathrm{d}t \ , & \text{if } T > T_\mathrm{def} \end{cases} \tag{5}$$

where the constant $\bar{\alpha}$ is a material parameter, T_def is the threshold of temperature above which DEF can be generated (about $65°C$), E_a^def is the activation energy relative to DEF expansion, and t_m is the maturation time (few days to few weeks depending on the size of the considered structure).

Now to take into account the influences of both of the thermal and hydric conditions, relation (4) must be adapted. To be exhaustive, let us assume the following choices that not all will be considered in this step of the developments due to the lack of experimental results.

2.1. Variable thermal conditions

It has been shown experimentally that the ambient temperature has an influence on the kinetics of expansion. Among other choices, we can consider that the two characteristic times be thermo-activated with the forms

$$\tau_l = \overline{\tau}_l \, e^{\left[\frac{U_l}{R}\left(\frac{1}{T}-\frac{1}{\overline{T}}\right)\right]}, \qquad \tau_c = \overline{\tau}_c \, e^{\left[\frac{U_c}{R}\left(\frac{1}{T}-\frac{1}{\overline{T}}\right)\right]}, \tag{6}$$

as suggested in [26, 28] for AAR. Here $\overline{\tau}_l$ and $\overline{\tau}_c$ are reference characteristic times for a reference temperature $\overline{T}$, and U_l and U_c are activation energies. Notice that, even possible, the amplitude ε_∞^0 is not affected by temperature in our DEF case.

2.2. Variable hydric conditions

Experimental evidences have also shown that the expansion stops below a certain threshold of humidity, see for example [19]. The relation (4) must then be adapted to take into account this strong dependency. In terms of saturation, denoting the threshold below which the expansion reaction stops by $\overline{S}_r$, we can formally write:

$$\begin{cases} \dot{\varepsilon}_\chi = 0 \ , & \text{if } S_r \leq \overline{S}_r \ , \\ \dot{\varepsilon}_\chi > 0 \ , & \text{if } S_r > \overline{S}_r \ , \\ \text{and } \varepsilon_\chi \text{ is given by (4)} \ , & \text{if } S_r = 1 \ . \end{cases} \tag{7}$$

Now for $\overline{S}_r < S_r < 1$, we need to establish a *continuous* link between the extreme situations $(7)_1$ and $(7)_3$. We introduce for this an *effective* time that we denote by $\widetilde{t}$ and such that,

$$\dot{\widetilde{t}} \equiv \dot{\widetilde{t}}(S_r, t, \ldots) \ \in \ [0, 1] \, . \tag{8}$$

A possible choice would be:

$$\dot{\widetilde{t}} = \left(\frac{\left\langle S_r - \overline{S}_r \right\rangle_+}{1 - \overline{S}_r} \right)^{\overline{m}} \qquad \Longrightarrow \qquad \widetilde{t} = \int_0^t \left(\frac{\left\langle S_r - \overline{S}_r \right\rangle_+}{1 - \overline{S}_r} \right)^{\overline{m}} \mathrm{d}t \,, \tag{9}$$

where the Macauley bracket $\left\langle \bullet \right\rangle_+$ denotes the positive part function, and the exponent parameter most probably depends on the saturation, i.e.

$$\overline{m} \equiv \overline{m}(S_r) \ . \tag{10}$$

Hence, by replacing the real time t by the effective time $\widetilde{t}$ into the expression (4), we obtain a free expansion law that covers the requirements (7) for variable humidity.

3. Constitutive equations and mechanical balance

The kinematic decomposition, Eq. (1), must now be embedded into a constitutive relation. At this point, the simplest choice is to consider an elastic relation for the reversible behaviour:

$$\boldsymbol{\sigma} = \mathbf{C} : \boldsymbol{\varepsilon}^{\mathrm{e}}, \tag{11}$$

where $\boldsymbol{\sigma}$ is the stress tensor and the elastic part of the strain tensor $\boldsymbol{\varepsilon}^{\mathrm{e}}$ is the one that has been used in the decomposition (1). $\mathbf{C}$ is the fourth-order elasticity tensor that can in turn be affected by chemical damage as

$$\mathbf{C} = (1 - d_\chi)\mathbf{C}_0 \,, \tag{12}$$

where $\mathbf{C}_0$ is the elastic modulus for the undamaged concrete (Hooke's law) and d_χ is a damage variable in the sense of contiuum damage mechanics, see for example [24, 29]. Intuitively, it can be driven by the chemical expansion

itself, then explicitly given as a function of the quantity ε_χ, for instance, the following form as adopted in [25]:

$$d_\chi = 1 - e^{\left[-\omega \left\langle \varepsilon_\chi - \varepsilon_{\text{trs}} \right\rangle_+\right]} , \tag{13}$$

where ε_{trs} is the strain-like chemical damage threshold below which no damage occurs, and $\omega \geq 0$ a convenient parameter, i.e. no chemical damage takes place if we take $\omega = 0$.

With (11) we have a minimalist modelling framework with the simplest possible resolution procedure. The mechanical balance is linear since the thermal and hydric fields are a priori known at every time step, i.e. assuming a weak coupling between the thermo-hydric diffusion and the mechanical equilibrium. Let us notice however that when inelastic strains (plasticity) will be taken into account together with creep and mechanical damage, the problem clearly becomes nonlinear. Furthermore, the thermal and hydric parts of the modelling are left out of the scope of this paper. Nevertheless, let us stress that for the hydric part at least, care must be taken when solving for the saturation field. Indeed, one the one hand, the hydric diffusion is not constant and, on the other hand, concrete materials are characterized by typical hysteretic sorption-desorption responses that strongly influence the soaking-drying kinetics, to mention a few. Developments on this topic are still in progress.

At the actual time t_{n+1} for instance, the weak form of the mechanical

balance at hand is given by:

$$\begin{aligned}\int_{\mathcal{B}} \nabla^{\mathrm{s}}\delta\boldsymbol{u} : \mathbf{C}_{n+1} : \nabla^{\mathrm{s}}\boldsymbol{u}_{n+1}\,\mathrm{d}V = G^{\mathrm{ext}}_{n+1}(\delta\boldsymbol{u}) \\ + \int_{\mathcal{B}} \nabla^{\mathrm{s}}\delta\boldsymbol{u} : \mathbf{C}_{n+1} : \left(\boldsymbol{\varepsilon}_{\mathrm{th}_{n+1}} + \boldsymbol{\varepsilon}_{\mathrm{hyd}_{n+1}} + \boldsymbol{\varepsilon}_{\chi_{n+1}}\right)\,\mathrm{d}V\ ,\end{aligned} \tag{14}$$

which must hold for any displacement variation $\delta\boldsymbol{u}$, and where $\nabla^{\mathrm{s}}(\centerdot)$ is the symmetric gradient operator. Here G^{ext}_{n+1} is a short hand notation for the virtual work of the external loads embedding both of the volumetric forces in the body $\mathcal{B}$ and traction forces on part of its boundary $\partial_{\boldsymbol{t}}\mathcal{B} \subset \partial\mathcal{B}$ applied at time t_{n+1}.

Equation (14) is to be solved for the actual displacement field $\boldsymbol{u}_{n+1}$. However, care must be taken in evaluating the chemical strain $\boldsymbol{\varepsilon}_{\chi_{n+1}}$ on the right hand-side of (14). Indeed, this latter is computed with the effective time $\widetilde{t}_{n+1}$ that must in turn be updated locally at each time step as:

$$\widetilde{t}_{n+1} = \widetilde{t}_n + \left(\frac{\left\langle S_{r_{n+1}} - \overline{S}_r\right\rangle_+}{1-\overline{S}_r}\right)^{\overline{m}_{n+1}} \Delta t\ , \tag{15}$$

where $\Delta t = t_{n+1} - t_n$ is the *real* time increment, and the exponent parameter $\overline{m}_{n+1}$ is evaluated with $S_{r_{n+1}}$, i.e. $\overline{m}_{n+1} \equiv \overline{m}(S_{r_{n+1}})$ in the form (10). Consequently, the effective time is treated as an internal field variable ; $\widetilde{t} \equiv \widetilde{t}(\boldsymbol{x}, t)$.

4. Simulations of the influence of the relative humidity on DEF expansions

In this section we present simulations with regards to experimental tests given in [19] on the study of the influence of relative humidity on expansion associated with DEF in concrete. A set of 11 × 22 cm cylindrical samples

made with a siliceous-based aggregate concrete were heat-treated at early age so as to potentially trigger DEF expansion, and then separated in different groups, each group submitted to a controled constant relative humidity RH, see [19] for details:

- Samples that have been stored at 94%, 96%, 98% and 100% RH, respectively denoted by RH94, RH96, RH98 and RH100. ;
- Samples that have been immersed continuously, denoted by IM ;
- Samples that have been stored at 91% RH and then immersed in water at the age of 334 days, denoted by RH91-IM.

The experimental results are shown in figure 1 where interesting observations are to be pointed out:

- Expansions under continuous immersion and RH100 (not shown here) are almost identical;
- With a relative humidity of 91%, the saturation is under the threshold $\overline{S}_r$;
- Above the saturation threshold, the expansion is very sensitive to the ambiant humidity, i.e. from 94 to 100% RH.

From the point of view of the modelling, the curve obtained at saturation $S_r = 1$ that corresponds to the case of RH100 or IM, is used to identify the parameters of the free-expansion law (4). They are summarized in Table 1 where the asymptotic parameters ϕ and δ are used for a better description of the long term expansion kinetics.

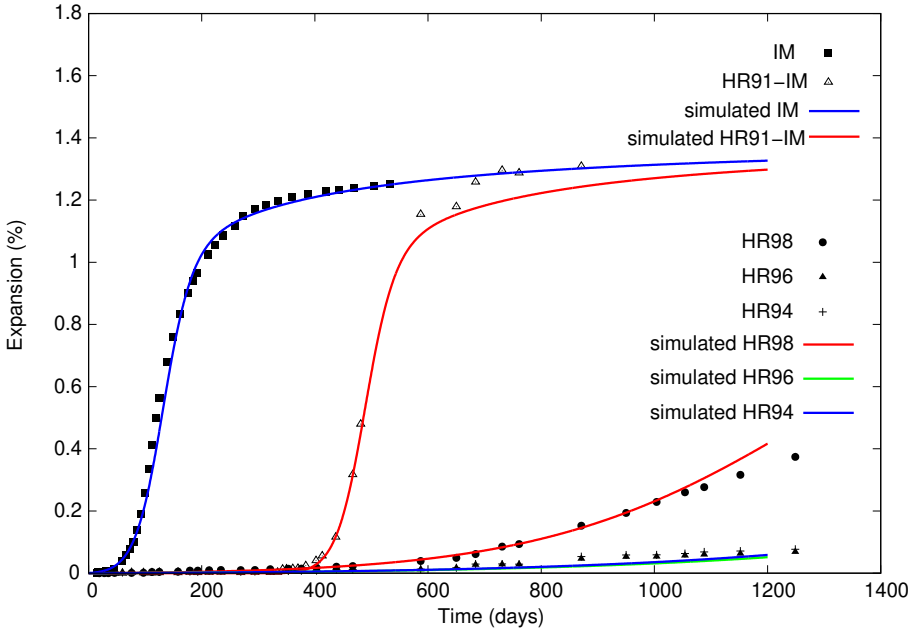

Figure 1: Expansions of all concrete specimens. Experimental results from (Al Shamaa & al., 2015). Superposition with the results of the numerical simulations.

Now for the effective time, the property $(7)_2$ is active in this example, so the expression (9) must be used. We take $\overline{S}_r = 0.93$ for the saturation threshold, and the exponent parameter $\overline{m}$ has the form (10) chosen here as a quadratic function given by,

$$\overline{m}(S_r) = 1 + 42.5(S_r - \overline{S}_r) + 1750(S_r - \overline{S}_r)^2 \ . \tag{16}$$

With this set of parameters at hand, we show in figure 1 the numerical results predicted by the model for the different exposures to humidity. One can notice that the model is able to represent the experimental behaviour.

Table 1: Material parameters with the expansion law (4) for the siliceous concrete of figure 1.

Definition	identified values
expansion amplitude ε_∞^0	1.4%
latent time τ_l	128 days
characteristic time τ_c	25 days
parameter ϕ	68 days
parameter δ	100 days

5. DEF expansions under cyclic soaking-drying cycles

An experimental compaign has been performed in this work as well. Concrete samples were designed for their known expansive behaviour when heat-treated and immersed in water after casting. The concrete formulation used is detailed in Table 2; A Portland cement CEMII/A L with 6% of calcareous additions (42.5 MPa) is used with a 0.57 water-cement ratio. Calcareous aggregates were used (Boulonnais aggregates).

Now to simulate the heating induced by cement hydration in massive structures, the samples undergo a thermic treatment as shown in figure 2: the temperature was maintained at $20°C$ for 2h, then increased from $20°C$ to $80°C$ in 24 h, then maintained at $80°C$ for three days, and then decreased from $80°C$ to $20°C$ in three days. After this treatment, half of the samples were immersed in water at $20°C$; the other half undergo soaking and drying cycles. In all cases, 11×22 cm cylindrical samples have been used, and are monitored following the LCPC method n°66.

Table 2: Concrete composition.

Materials	Composition
Cement	350 kg
Water	210 kg
Sand (0-5 mm)	858 kg
Aggregates (5-12.5 mm)	945 kg
Viscosity modifying admixture	6.6 kg
W/C	0.57
A/S	1.1
Density	2354 kg/m^3

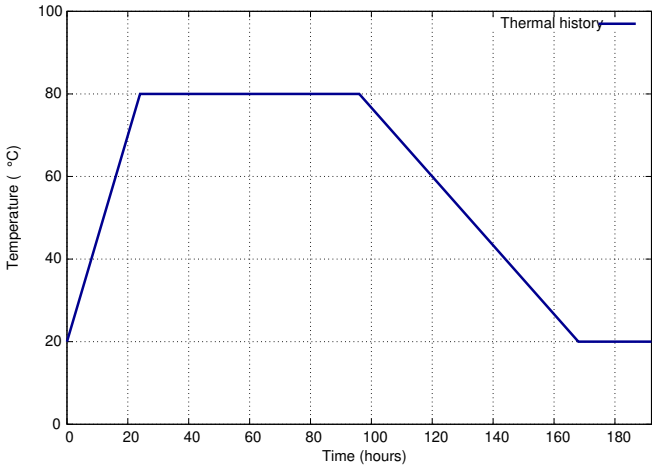

Figure 2: Heating treatment of the 11×22 cm cylindrical samples during first hours after curing.

5.1. Simulations for the immersed samples

The experimental evolution of the mean expansions for the samples is presented in figure 3, in square-dots-points. The phase of accelerated degradation is finishing and the stabilisation phase is taking place (about 0.23% maximum expansion).

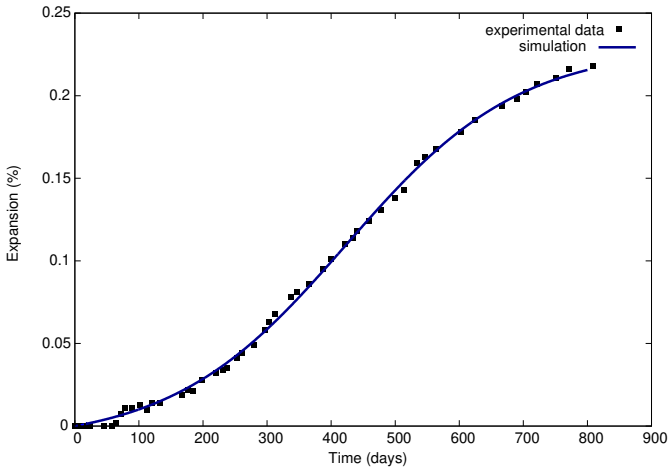

Figure 3: Swelling of concrete samples with calcareous aggregates. Experimental data and numerical simulation.

Curve fitting with the free-expansion law (4) gives the parameters summarized in Table 3 where Larive's law is sufficient, i.e. with $\phi = 0$.

With these values, the simulated expansion is superposed in figure 3 where a good agreement is to be noticed. As the samples are immersed during the whole time, uniform saturation $S_r = 1$ is taken and, consequently, the effective time is identical to the real time.

Table 3: Material parameters with the expansion law (4) for the calcareous-based concrete.

Definition	identified values
expansion amplitude ε_∞^0	0.23%
latent time τ_l	423.5 days
characteristic time τ_c	135.48 days
parameter ϕ	0
parameter δ	0

5.2. Simulations of the effect of soaking-drying cycles on DEF

A second set of samples with the above calcareous aggregates was submitted to cycles of drying (at 50 % of relative humidity and $23°C$) alternated with soaking (at $23°C$) to represent a more realistic environment of some structures which are not permanently in contact with water. The cycles are recorded in Table 4.

The swelling monitoring of this new study is plotted in figure 4 (the dashed line with circle dots), and compared to the previous experimental curve of figure 3 with the samples kept continuously immersed in water (square-dots-points curve). One can notice that the drying cycles restrict the delayed ettringite formation in the material and have an important impact on the expansion kinetics.

From the modelling point of view, this falls within the scope of the properties $(7)_1$ for drying, and $(7)_3$ for soaking. For the material parameters of the expansion law (4), we use the ones of Table 3. And for the effective time (9), we fix the saturation threshold to $\overline{S}_r = 0.95$. Here the computation is

Table 4: Soaking-drying cycles for the calcareous-based concrete samples.

Cycle n°	Soaking time *(days)*	Drying time *(days)*
1	9	14
2	22	20
3	7	7
4	10	12
5	20	12
6	35	9
7	22	22
8	10	7
9	23	19
10	16	7
11	34	10
12	19	21
13	13	22
14	12	7
15	37	22
16	13	21
17	13	17
18	38	23
19	41	24
20	14	17
21	30	20
22	38	38
23	42	24

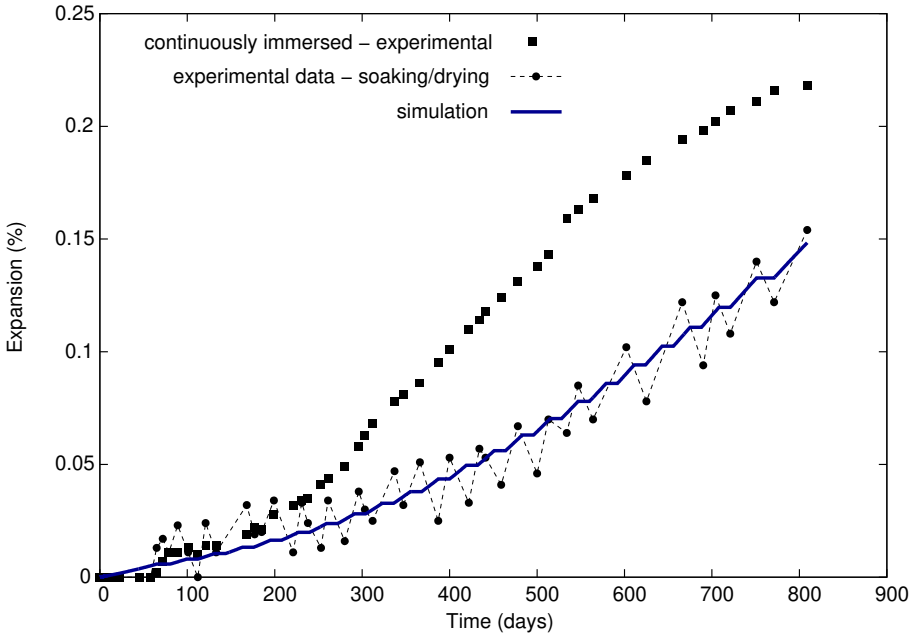

Figure 4: Impact of drying cycles on the swelling of concrete samples with calcareous aggregates. Experimental data and numerical simulation.

independent of the exponent parameter $\overline{m}$ since:

$$\dot{\widetilde{t}} = \begin{cases} 1 & \text{for soaking, with } S_r = 1\,, \\ 0 & \text{for drying, since } S_r \ll \overline{S}_r\,. \end{cases} \tag{17}$$

In the numerical computation, uniform saturation $S_r = 1$ is taken during the first 72 days, then cycles of drying for 13 days at $S_r = 0.48$ followed by soaking for 19 days at $S_r = 1$ are prescribed. In total, the sample is immersed 514 days and dried 295 days.

The simulated expansion is superposed in figure 4 where good agreement is again observed. Notice further that the expansion after 809 days of alternate soaking/drying cycles is almost the same as the 514 days' expansion in continuous immersion conditions.

6. Conclusions

In this study, we have presented and numerically tested an efficient tool for the modelling of the influence of relative humidity on the development of DEF expansions. The simple notion of effective time implicitly takes into account the amount of water during time in variable environmental conditions that strongly influence the kinetics of DEF expansions.

From the numerical point of view, we have briefly presented a numerical design for the integration of the chemical strain and the update of the effective time. In particular, this latter must be performed at the integration points level when use is made of the finite element method.

Numerical simulations have shown good agreements with the experimental results issued from an experimental compaign, and others from the literature. However, further studies are ongoing to include this notion within more detailed and complex formulations, i.e. including creep, plasticity and mechanical damage among others.

Bibliography

[1] H. F. W. Taylor, C. Famy, K. L. Scrivener, Delayed ettringite formation, Cement and Concrete Research 31 (2001) 683–693.

[2] M. Al Shamaa, S. Lavaud, L. Divet, G. Nahas, J.-M. Torrenti, Coupling between mechanical and transfer properties and expansion due to DEF in a concrete of a nuclear power plant, Nuclear Engineering and Design 266 (2014) 70–77.

[3] M. M. Karthik, J. B. Mander, S. Hurlebaus, Experimental behavior of large reinforced concrete specimen with ASR and DEF deterioration, Journal of Structural Engineering 144(8) (2018) : 04018110.

[4] A. Pavoine, X. Brunetaud, L. Divet, The impact of cement parameters on delayed ettringite formation, Cement and Concrete Composites 34 (2012) 521–528.

[5] I. Odler, Y. Chen, Effect of cement composition on the expansion of heat-cured cement pastes, Cement and Concrete Research 25 (1995) 853–862.

[6] S. Kelham, The effect of cement composition and fineness on expansion associated with delayed ettringite formation, Cement and Concrete Composites 18 (1996) 171–179.

[7] X. Brunetaud, R. Linder, D. Duragrin, D. D., Effect of curing conditions and concrete mix design on the expansion generated by delayed ettringite formation, Materials and Structures 40 (2007) 567–578.

[8] P. J. M. Monteiro, P. K. Mehta, The tranzition zone between aggregate and type k expansive cement, Cement and Concrete Research 16 (1986) 111–114.

[9] P. E. Grattan-Bellew, J. J. Beaudoin, V. G. Vallee, Effect of aggregate particle size and composition on expansion of mortars bars due to delayed ettringite formation, Cement and Concrete Research 28(8) (1998) 1147–1156.

[10] X. Brunetaud, Etude de l'influence de différents paramètres et de leurs intéractions sur la cinétique et l'amplitude de la réaction sulfatique interne, Phd thesis, Ecole Centrale de Paris (2005).

[11] M. Al Shamaa, S. Lavaud, L. Divet, J. B. Colliat, G. Nahas, J.-M. Torrenti, Influence of limestone filler and of the size of the aggregates on def, Cement and Concrete Composites 71 (2016) 175–180.

[12] C. D. Lawrence, Mortar expansions due to delayed ettringite formation. Effect of curing period and temperature, Cement and Concrete Research 25 (1995) 903–914.

[13] B. Kchakech, Etude de l'influence de l'échauffement subi par un béton sur le risque d'expansions associées à la réaction sulfatique interne, Phd thesis, Université Paris-Est (2015).

[14] A. E. Moore, H. F. W. Taylor, Crystal Structure of Ettringite, Acta Crystallographica 26(4) (1970) 386–393.

[15] C. Famy, K. L. Scrivener, A. Atkinson, A. R. Brough, Influence of the storage conditions on the dimensional changes of heat-cured mortars, Cement and Concrete Research 31 (2001) 795–803.

[16] D. Heinz, U. Ludwig, I. Rüdiger, Delayed ettringite formation in heat treated mortars and concretes, Concrete Precasting Plants and Technology 11 (1989) 56–61.

[17] L. Graf, Effect of relative humidity on expansion and microstructure of heat-cured mortars, Portland Cement Association (2007) 50.

[18] R.-P. Martin, Experimental analysis of the mechanical effects of delayed ettringite formation on concrete structures, Phd thesis, Université Paris-Est (2010).

[19] M. Al Shamaa, S. Lavaud, L. Divet, G. Nahas, J.-M. Torrenti, Influence of relative humidity on delayed ettringite formation, Cement and Concrete Composites 58 (2015) 14–22.

[20] M. M. Karthik, J. B. Mander, S. Hurlebaus, ASR/DEF related expansion in structural concrete: model developments and validation, Construction and Building Materials 128 (2016) 238–247.

[21] A. Sellier, S. Multon, Chemical modelling of delayed ettringite formation for assessment of affected concrete structures, Cement and Concrete Research 108 (2018) 72–86.

[22] M. M. Karthik, J. B. Mander, S. Hurlebaus, Modeling ASR/DEF expansion strains in large reinforced concrete specimens, Journal of Structural Engineering 144(7) (2018) : 04018085.

[23] B. Nedjar, A time dependent model for unidirectional fibre-reinforced composites with viscoelastic matrices, International Journal of Solids and Structures 48 (2011) 2333–2339.

[24] B. Nedjar, R. Le Roy, An approach to the modeling of viscoelastic damage. Application to the long-term creep of gypsum rock materials, International Journal for Numerical and Analytical Methods in Geomechanics 37 (2014) 1066–1078.

[25] N. Baghdadi, Modélisation du couplage chimico-mécanique d'un béton atteint d'une réaction sulfatique interne, Phd thesis, Université Paris-Est (2008).

[26] C. Larive, Apports combinés de l'expérimentation et de la modélisation à la compréhension de l'alcali-réaction et de ses effets mécaniques, Laboratoire Central des Ponts et Chaussées, OA 28, 1998.

[27] J.-F. Seignol, N. Baghdadi, F. Toutlemonde, A macroscopic chemo-mechanical model aimed at re-asseeement of def-affected concrete structures, in: International Conference on Computational Technologies in Concrete Structures, CTCS'09, Korea, 2009, pp. 422–440.

[28] S. Poyet, Etude de la dégradation des ouvrages en béton atteints par la réaction alcali-silice : Approche expérimentale et modélisation numérique multi-échelle des dégradations dans un environnement hydro-chemo-mécanique variable, Phd thesis, Université de Marne-la-Vallée (2003).

[29] B. Nedjar, On a concept of directional damage gradient in transversely isotropic materials, International Journal of Solids and Structures 88-89 (2016) 56–67.